

Long-Time Relaxations in Rubber-Modified Polymer Systems

Yuji Aoki

Chemical Science Laboratories, Mitsubishi Chemical Corporation, 1, Toho-cho, Yokkaichi, Mie 510-8530, Japan

SUMMARY: Linear and nonlinear viscoelastic properties were measured in the molten state for several model ABS polymers with different rubber particle contents. Linear viscoelastic functions for ABS polymers can be separated in two parts. One is a relaxation associated with the entanglement of matrix SAN chains and the other comes from the particle-particle interactions of rubber particles. This relaxation depends strongly on the degree of dispersion of rubber particles. The second-plateau modulus appeared at low frequency with samples in which rubber particles agglomerate. While, the second-plateau modulus was not observed with samples in which rubber particles are finely dispersed. Matching of AN content between grafted and matrix SAN and optimum graft density form a finely dispersed system. Large deformation relaxation measurements revealed that the damping of ABS polymers having a good dispersion of particles become stronger with an increase in rubber content. This strong damping can be explained by a layered structure. The very long relaxation was found for higher rubber content, when the neighboring grafted SAN chains contact with each other.

Introduction

Many kinds of rubber-modified thermoplastic polymers have been developed and used in industrial fields. By blending of rubber component to rigid polymers, impact strength of the polymer is improved, while the other properties are usually deteriorated and the processability is changed. Therefore, it is very important for development of rubber-modified polymers to find how to improve the impact strength without deterioration of the rheological properties.

Acrylonitrile-butadiene-styrene (ABS) polymers are one of the most typical rubber-modified polymers commercialized at about 4 decades ago. Manufacturing of ABS polymers first was made by blending of poly(styrene-co-acrylonitrile) (SAN or AS) and rubber. Nowadays, ABS polymers of graft type are made by copolymerizing styrene and acrylonitrile monomers in the presence of rubber. During the polymerization some of the SAN become grafted to the rubber. The grafted SAN acts as a dispersing agent. Therefore, ABS polymers consist of a continuous SAN in which the rubber phase (polybutadiene grafted with SAN) is dispersed in the form of spherical particles. Physical properties of ABS polymers are influenced by not only the rubber content, rubber particle size, and molecular weight of the matrix SAN, but also the quantity, composition, and molecular weight of the grafted SAN on the surface of rubber particles.

In this study, we prepared several model ABS polymers by emulsion polymerization and mixed with SAN to obtain ABS polymers with various rubber contents. We studied dynamic viscoelastic and shear stress relaxation properties of the polymers in the molten state in order to clarify the relationship between structure and rheological properties of ABS polymers.

Characteristic Features of the Linear Viscoelastic Properties

First, the linear viscoelastic properties of ABS polymer melts were investigated. The master curves of the storage shear modulus G' and loss modulus G'' for the two types of ABS polymers (ABS-A and ABS-B) as well as the matrix polymer (SAN) are shown in Fig.1¹⁾. The curves were obtained by horizontal shifting the G' and G'' versus frequency curves measured at various temperatures. The weight average molecular weight (M_w) and AN % of the matrix SAN (AS-1) is 5.75×10^4 and 25 wt %, respectively, for all the samples measured. ABS-A has a broad distribution of rubber particle size and ABS-B has a relatively narrow distribution. The grafting degree (Gd; defined by weight fraction of grafted SAN to rubber particles) is 0.37 and 0.85 for ABS-A and ABS-B, respectively. In these figures, the numbers (10, 20, 30) near the data lines indicate the weight % of the rubber particles. The reference temperature is 170 °C. The general characteristic features of the viscoelastic functions for ABS polymers can be clearly seen and divided into two regions from these figures. The first is the rubbery plateau regions at which both G' and G'' extend to the lower frequency side (long time scales) with increasing rubber content, suggesting the relaxation time becomes longer due to the presence of particles. This relaxation found for ABS-A and ABS-B is associated with the entanglement relaxations

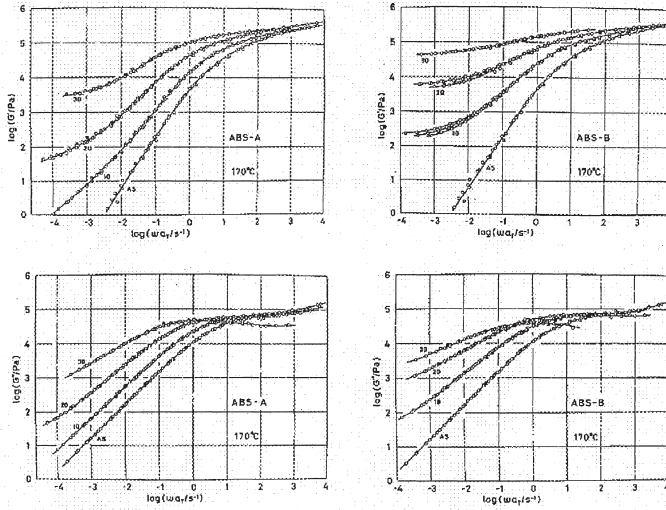


Fig.1: Master curves of the storage modulus G' and the loss modulus G'' for ABS-A and ABS-B with different rubber contents at 170 °C¹⁾.

of matrix SAN. The second is the most remarkable viscoelastic behavior of ABS polymers in the lower frequency region. G' curves for ABS-B exhibit the “second plateau”, which was first named for dispersed systems of solid particles in polymer liquids²⁾. The second plateau becomes clear and the intensity becomes higher with increasing rubber content. A complete application of the time-temperature superposition on the G' function fails at low frequencies where the second plateau appears for ABS-B. On the other hand, G' of ABS-A decreases with a lowering of frequency and the second plateau cannot be observed. The second plateau regions of G' and G'' for ABS-A and ABS-B are compared with each other in Fig.1. The plateau modulus of ABS-B is much higher than that of ABS-A. Fig. 2 shows electron micrographs of ABS-A and ABS-B¹⁾. Microscopic observations exhibit that rubber particles in ABS-A are finely dispersed without agglomeration, while rubber particles in ABS-B agglomerate in the matrix phase and form three-dimensional network structure. It is concluded that the viscoelastic functions and the second plateau modulus are significantly affected by the degree of dispersion of rubber particles in the matrix SAN. A relationship between the degree of

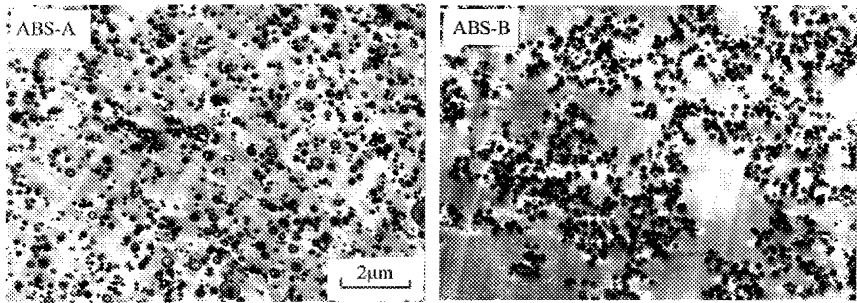


Fig.2: Electron microscopic photographs of ABS-A-10 and ABS-B-10 after viscoelastic measurement¹⁾.

dispersion of rubber particles and chemical structure of ABS polymers will be discussed in the next section.

Effects of Composition and Amount of Grafted SAN

In this section, the effects of chemical composition and amount of the grafted SAN on the

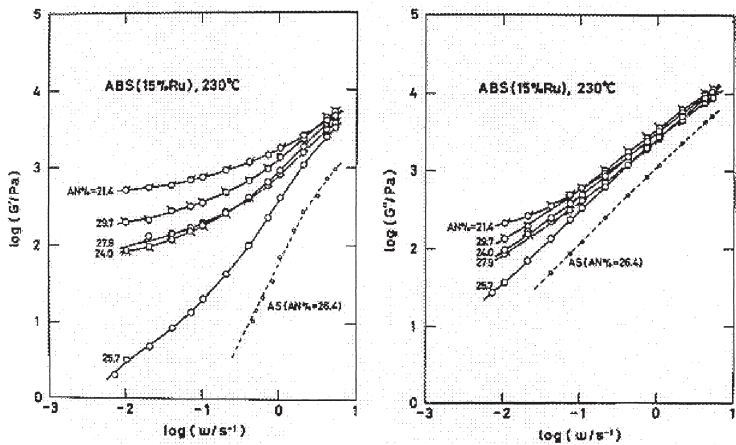


Fig. 3: Frequency dependence of the storage modulus G' and the loss modulus G'' for ABS with different acrylonitrile content of grafted SAN at 230°C³⁾.

viscoelastic properties were investigated³⁾. Fig. 3 shows the G' and G'' for ABS with different AN content of grafted SAN measured at 230 °C. The molecular weight of the grafted SAN is almost same as the matrix phase. AN % of the grafted SAN is varied from 21.4 to 29.7. The G' at low frequency strongly depends on AN % of the grafted SAN. The values of G' at $\omega = 1.05 \times 10^{-2} \text{ s}^{-1}$ are plotted against AN % of the grafted SAN in Fig. 4. The arrow indicates the position of AN % of the matrix SAN of 26.4 %. It is clear that the G' value takes a minimum when AN % of the matrix SAN and of the grafted one are the same and a small deviation of AN % makes a great increase of G' . When the AN % of matrix and grafted SAN is different, an agglomeration of particles is observed by electron microscope and a higher-order structure of particles produces a high value of the second plateau modulus. The mismatching of AN % between the matrix and grafted SAN caused the agglomeration of rubber particles and led to the observation of second plateau in these ABS polymers.

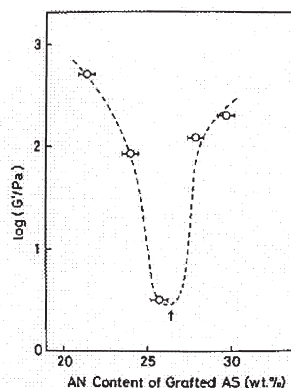


Fig. 4: Storage modulus G' at $\omega = 1.05 \times 10^{-2} \text{ s}^{-1}$ plotted against acrylonitrile content of grafted SAN. Arrow denotes acrylonitrile content of matrix SAN³⁾.

Next, we discuss the effect of grafting degree on the state of dispersion of particles for ABS polymers having two kinds of particle sizes^{4),5)}. Fig. 5 shows the master curves of G' for ABS having different grafting degree (Gd) at 200 °C. The rubber content is 20 % and rubber particle size is 350 nm. The G' does not depend much on the grafting degree at high frequencies. However, the G' becomes higher with an increase in the grafting degree in low frequency regions. For the ABS of low degree of grafting, the G' decreases with a lowering of frequency, while for the ABS of high grafting degree the second-plateau is attained at low frequency. In order to elucidate grafting degree dependence of the viscoelastic functions, the values of G' at 200 °C and $1.05 \times 10^{-2} \text{ s}^{-1}$ are plotted against grafting degree. The results are shown in Fig. 6. In this figure, the data for ABS polymers having rubber particle size of 170 nm reported previously⁴⁾ were added. It is clear that the

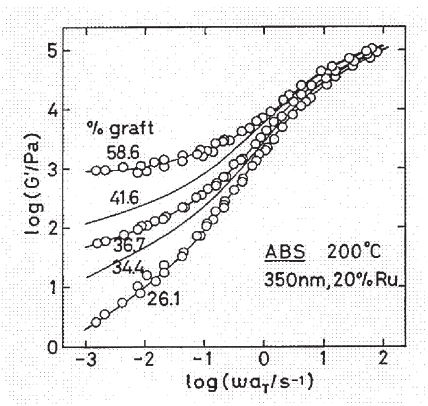


Fig. 5: Master curves of the storage modulus G' for ABS having different grafting degree at 200 °C.

viscoelastic functions first decrease and then increase with an increase in the grafting degree. The minimum in the functions occurred at the grafting degree of about 40 % and 20 % for ABS polymers having rubber particle size of 170 and 350 nm, respectively. When the grafting degree is below or above 40 % and 20 %, second-plateau regions are observed in the long time region. Electron microscopic observation revealed that the sample having Gd of 41.3 % shows a good dispersion of rubber particles and the other samples show the agglomeration of the rubber particles. The degree of agglomeration becomes remarkable for the sample having high Gd. The same result was observed for the samples with particle size of 350 nm. We found that the rubber particles of samples having the minimum in the viscoelastic functions are finely dispersed but that those of the other samples exhibiting second plateau form an agglomerated or three-dimensional network

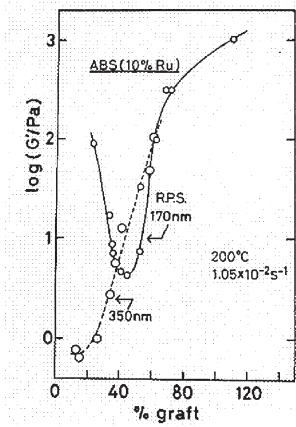


Fig. 6: Storage modulus G' of ABS polymers at $\omega = 1.05 \times 10^{-2} \text{ s}^{-1}$ plotted against %graft at 200 °C.

structure of rubber particles.

The above facts show that there is an optimum graft density for dispersing the rubber particles. Because, the graft density, which is defined as the number of polymers per unit surface area of the rubber particles, is proportional to $G_d \cdot D$, where D is the particle diameter, and the graft density at the minima in G' is same for two ABS polymers. Recently, Hasegawa et al. calculated the interaction free energy between two polymer grafted plates in polymer melt separated by distance H using a mean field approximation⁵⁾. They assume that all the polymers are made of the same monomers. The excess surface free energy F_s of the systems per unit area of the plate was calculated. The interaction energy $A_{pol}(H)$ between two spherical particles with diameter D separated by distance H was calculated by using Derjagin approximation. The actual interaction $A_{int}(H)$ is the sum of $A_{pol}(H)$ and van der Waals attraction $A_{vdw}(H)$. The parameter used in this calculation was taken as almost same as our experiment. In all cases, $A_{int}(H)$ has attractive part, and the minimum of the attraction part varies with graft density σ . The optimum graft density corresponds to σ which gives the least depth of the attraction. This corresponds to $\sigma = 0.1 \text{ nm}^{-2}$, which compares well with the optimum graft density. Also notice that the optimum graft density is independent of the particle diameter. This is the reason of the optimum graft density.

Rheological Properties of ABS Polymer Melts having a Good Dispersion of Rubber Particles

We investigated dynamic viscoelastic and steady-flow properties of ABS polymers in which rubber particles were well dispersed without agglomeration^{6), 7)}. Two series of ABS polymers (ABS-C and ABS-D) were used in this work. The number-average particle diameter for ABS-C and ABS-D is 350 and 170 nm, respectively. Both samples have very narrow distribution of rubber particle size. The grafting degree is 0.20 and 0.41 for ABS-C and ABS-D, respectively. SAN of the matrix is the same as used for ABS-A and ABS-B. Fig. 7 shows the experimental data of dynamic and steady-state rheological properties of ABS-C and ABS-D as well as the matrix SAN at iso-free volume fraction of $f = 0.0797$. Open circles indicate the shear stress σ and closed circles the absolute value of complex shear modulus $|G^*| = (G'^2 + G''^2)^{1/2}$. It is evident that $|G^*|$ is in excellent agreement with σ for C-10, C-20, D-5, D-10, and D-15 samples in all the regions of shear rate and frequency measured. This result confirms that Cox and Merz's empirical rule⁸⁾

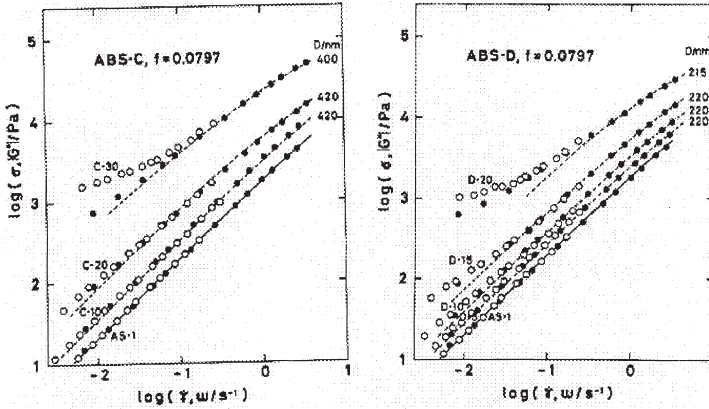


Fig. 7: Shear rate dependence of shear stress σ (○) and frequency dependence of complex shear modulus $|G^*|$ (●) for ABS-C and ABS-D having different rubber content at $f = 0.0797$. Dotted lines denote the calculated flow curves by a layered structure model⁷⁾.

holds well for ABS polymers in the low shear and low frequency region. For the present samples without agglomeration, the yield stress cannot be observed and the deviation from Newtonian flow is relatively small. $|G^*|$ and σ increase with an increase in rubber content. Comparison of flow curves of ABS-C and ABS-D indicates that $|G^*|$ and σ of ABS-D are higher than those of ABS-C having larger particle size at the same rubber content. For the samples of the highest rubber content (C-30 and D-20) of each series, $|G^*|$ does not agree with σ , and the non-Newtonian behavior becomes remarkable and yield stress is observed at low shear rates. The grafted chains on one particle may be in contact with, or entangled with, those on the neighboring particles for the samples.

In order to explain the effect of the particle size on the flow curves for ABS polymers, we proposed a layered structure model shown in Fig.8. In this model, the rubber particles are arranged perpendicular to the velocity gradient and form a layered structure, and rubber particles in a layer are assumed to be packed tetragonally. The layered structure is a model that resistance by dispersed particles in the flow field is reduced to a minimum. Since the storage modulus of the rubber is high, about $4 \times 10^5 \text{ Pa}$ ⁹⁾, rubber particles cannot be deformed for low shear rate. Then, the value of velocity gradient in the particle layers under shear is zero. When a fully developed shear flow is assumed in the fluid between

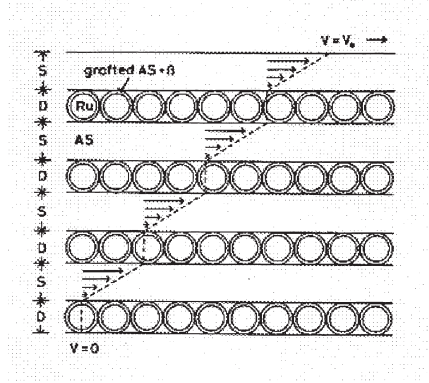


Fig. 8: A model for ABS polymer melts under simple shear. Velocity is given by V . S is the thickness of a fluid layer and D is the thickness of an immobile region including grafted SAN⁷⁾.

the particle layers, the actual shear rate between the layers becomes $(1 + D/S)$ times, where D is the thickness of the particle layer and S that of the fluid layer. If the medium is a Newtonian fluid, shear stress also increases $(1 + D/S)$ times. The calculated flow curves are denoted by the dotted lines in Figure 7. In these calculated curves, we assume $D = 420$ nm for C-10 and C-20, 400 nm for C-30, 220 nm for D-5, D-10, and D-15, and 215 nm for D-20, as shown in the figure. All the calculated curves are then in good agreement with experimental values. However, this model cannot explain non-Newtonian flow in the very long time region.

Next, we investigated large deformation stress relaxation measurements for the ABS polymers having good dispersion of rubber particles. The particle diameter of the ABS-T(3) used in this experiment is about 300 nm. Distribution of rubber particle size is not so narrow comparing with ABS-C and ABS-D. The grafting degree is 0.98. This value is large, because ABS-T(3) includes many occluded SAN besides grafted SAN. Rubber content is 6, 10, 15, 17.5, and 20 wt %. The weight average molecular weight and AN % of the matrix SAN (SAN-29) is 7.7×10^4 and 29.2 wt %, respectively. AN % of the grafted SAN was almost equal to that of SAN-29. Oscillatory shear and step-shear stress relaxation measurements were carried out with a laboratory rheometer (ARES,

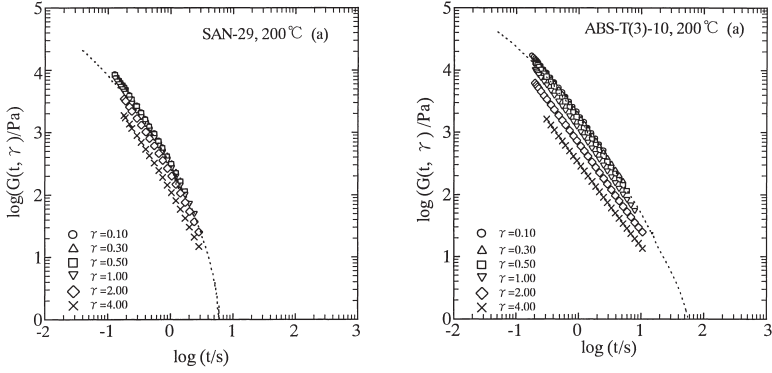


Fig. 9: Stress relaxation modulus $G(t, \gamma)$ obtained at various strains γ for SAN-29 (left) and ABS-T(3)-10 (right) at 200 °C. The dotted line is the linear relaxation modulus curve calculated from the dynamic viscoelastic data.

Rheometrics). At first, we checked time sweeps of G' and G'' at 240 °C and frequency of 0.04 rad/s on the 6 % rubber content sample (ABS-T(3)-06). An increase of G' and G'' with time was not observed. No agglomeration of rubber particles could be detected by transmission electron microscope. These facts confirm that ABS-T(3) systems have good dispersion of rubber particles. Fig. 9 shows the strain-dependent relaxation modulus $G(t, \gamma)$ for SAN-29 and ABS-T(3)-10, respectively, at 200°C. The shear strain measured ranges from 0.01 to 4.5. The dotted curve represents the linear relaxation modulus $G(t)$ calculated from the G' and G'' data by the method of Ninomiya and Ferry¹⁰.

$$G(t) = [G'(\omega) - 0.4G''(0.4\omega) + 0.014G''(10\omega)]_{\omega=1/t} \quad (1)$$

The relaxation modulus curves obtained at the strains from 0.01 to 0.50 for SAN-29 are very close each other and agree with the linear relaxation curve. The relaxation modulus $G(t, \gamma)$ decreases with an increase in strain and nonlinearity becomes stronger. Compared with that of SAN-29, the whole relaxation curve of ABS-T(3)-10 at each strain shifts to the longer time scale. It seems that a long-time relaxation mechanism due to the particles emerges. The γ dependence of $G(t, \gamma)$ for T(3)-10 is stronger than that for SAN-29. The curves at various strains could be superposed by vertical shifts in the time range covered by this experiment. Then, $G(t, \gamma)$ can be factorized at long times as

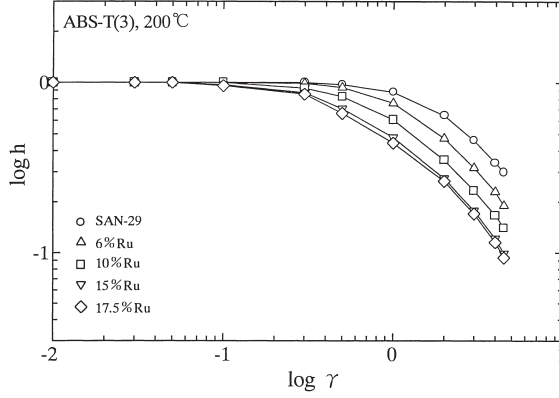


Fig. 10: Damping functions $h(\gamma)$ obtained from stress relaxation modulus of SAN-29 and ABS polymers having different rubber content.

$$G(t, \gamma) = G(t)h(\gamma) \quad (2)$$

where, $G(t)$ is the linear stress relaxation modulus and $h(\gamma)$ is the damping function. The damping functions were calculated based on the experimental relaxation modulus. It was not applicable for ABS-T(3)-20 sample, as Masuda et al.¹¹⁾ already found that the strain dependence of the relaxation modulus for ABS polymer melts disappears in the region where a long-time relaxation due to the particle-particle interactions is dominant. Fig. 10 illustrates the damping functions of ABS samples with various rubber contents from 0 to 17.5 %. The damping function of ABS polymers became stronger with increasing rubber content. For stress relaxation in shear, the damping function can be expressed by

$$h(\gamma) = 1/(1 + a\gamma^2) \quad (3)$$

The damping function of SAN-29 is very similar to polystyrene. Evaluating a value of SAN-29 from best fit with eq. (3) is 0.132. This value is in good agreement with the value of $a=0.142$ for broad molecular weight distribution polystyrene ($M_w/M_n=2.5$)¹²⁾. What is the reason why ABS polymers have stronger damping than matrix SAN does ? We can consider that the received strain in matrix SAN molecules is much larger than that of the applied strain from outside as described in Fig. 8. The deformation (effective strain) can be generated in only the SAN matrix, because rubber particles do not receive

any deformation. The strong damping of ABS polymers can be explained by the above model.

Conclusion

The linear and nonlinear viscoelastic properties have been investigated for several model ABS polymers with various rubber particle contents. Linear viscoelastic functions for ABS polymers can be separated in two parts. One is a relaxation associated with the entanglement of matrix SAN chains, which shifts to a longer time with increasing rubber content. The other is found at a longer time region and comes from the particle-particle interactions of neighboring rubber particles. This relaxation depends strongly on the degree of dispersion of rubber particles. With samples in which rubber particles agglomerated and formed three-dimensional network structure, the second-plateau modulus appeared in plots of storage modulus G' against frequency at low frequency. While, the second-plateau modulus was not observed with samples in which rubber particles were finely dispersed, and values of G' decreased with lowering frequency. Matching of AN content between grafted and matrix SAN and optimum graft density form a finely dispersed system.

For ABS polymers having a good dispersion of rubber particles, the relaxation mechanism associated with the entanglement of matrix SAN can be explained by a model in which rubber particles are arranged in layers. Large deformation relaxation measurements revealed that the damping of ABS polymers became stronger with an increase in rubber content. This strong damping also can be explained by the layered structure. The very long relaxation was found for higher rubber content when the neighboring grafted SAN chains overlap or contact with each other.

References

1. Y. Aoki, *J. Soc. Rheol. Jpn.* **7**, 20 (1979)
2. S. Onogi, T. Masuda, T. Matsumoto, *Trans. Soc. Rheol.* **14**, 275 (1970)
3. Y. Aoki, K. Nakayama, *J. Soc. Rheol. Jpn.* **9**, 39 (1981)
4. Y. Aoki, *Macromolecules* **20**, 2208 (1987)
5. R. Hasegawa, Y. Aoki, M. Doi, *Macromolecules* **29**, 6656 (1996)
6. Y. Aoki, K. Nakayama, *Polymer J.* **14**, 951 (1982)
7. Y. Aoki, *J. Non-Newt. Fluid Mech.* **22**, 91 (1986)

8. W. P. Cox, E. H. Merz, *J. Polym. Sci.* **28**, 619 (1958)
9. T. Masuda, A. Nakajima, M. Kitamura, Y. Aoki, N. Yamauchi, A. Yoshioka, *Pure Appl. Chem.*, **56**, 1457 (1984)
10. J. D. Ferry, *Viscoelastic Properties of Polymers*, 3rd ed., Wiley, New York 1980
11. M. Takahashi, L. Li, T. Masuda, *J. Rheol.* **33**, 709 (1989)
12. M. Takahashi, O. Urakawa, N. G. Ebrahimi, T. Isaki, T. Masuda, *J. Soc. Rheol. Jpn.* **24**, 37 (1996)